Eur. Phys. J. B **45**, 443–448 (2005)
DOI: 10.1140/epjb/e2005-00206-4

THE EUROPEAN PHYSICAL JOURNAL B

Saddle-point energies and Monte Carlo simulation of the long-range order relaxation in CoPt

M. Allalen[1,2,a], H. Bouzar[2], and T. Mehaddene[3]

[1] Universität Osnabrück, Fachbereich Physik, 49069 Osnabrück, Germany
[2] LPCQ, University M. Mammeri, 15000 Tizi-Ouzou, Algeria
[3] Physik Department E13/FRM II, TU München, 85747 Garching, Germany

Received 9 September 2004 / Received in final form 11 January 2005
Published online 13 July 2005 –

Abstract. We present atomic-scale computer simulations in equiatomic $L1_0$-CoPt where Molecular Dynamics and Monte Carlo techniques have both been applied to study the vacancy-atom exchange and kinetics relaxation. The atomic potential is determined using a Tight-Binding formalism within the Second-Moment Approximation. It is used to evaluate the different saddle-point energies involved in a vacancy-atom exchange between nearest-neighbour sites. The potential and the saddle-point energies have been used to simulate the relaxation of the long-range order in CoPt using a Monte Carlo technique. A vacancy migration energy of 0.73 ± 0.15 eV and an order-disorder transition temperature of 935 K have been found.

PACS. 61.43.Bn Structural modeling: serial-addition models, computer simulation – 64.60.Cn Order-disorder transformations; statistical mechanics of model systems – 66.30.Fq Self-diffusion in metals, semimetals, and alloys

1 Introduction

Ordering kinetics in intermetallic compounds have been the topic of many experimental and theoretical works. Systems presenting a phase diagram derived from the Au–Cu canonical phase digram are among the most studied. Owing to their high magnetic anisotropy, some of them in the iron-group metals and platinum group metals are of outstanding technological importance [1–5]. A good knowledge of the ordering process and its dynamics is thus a necessary step in any extensive research on these systems. Among the energetic parameters that drives diffusion, the saddle-point energies and the migration energies are generally less known and hard to measure in ordered intermetallic compounds. In pure metals and random alloys, the migration energy can be deduced, for example, from stage III of resistivity recovery during annealing after low-temperature irradiation [6] or thorough analysis of residual resistometry along isothermal and isochronal annealing series [7,8]. Those two methods are, however, very sensitive to the microstructure of the samples and to any impurities or defects. Based on the earlier work of Flynn [9], Schober et al. [10] have proposed a model for determining the migration energy from the phonon density of states in pure fcc and bcc metals. This model has been extended latter on to AB_3 compounds with $L1_2$ structure [11]. A prerequisite for such a determination is the knowledge of the phonon dispersion at different temperatures and states of order. In parallel to these experimental approaches, computer simulations, based on Molecular Dynamics (MD) and Monte Carlo (MC) techniques, allow one a wide range of kinetics relaxation problems and thermodynamic properties to be studied. Offering a possibility for investigating atomic migration in terms of crystal energetics treated by means of advanced solid-state theories, MD simulations are, however, technically limited to rather small samples and short periods of real time. Consequently, being very powerful when considering the dynamics of single atoms in a solid [12], the method is less useful for studying net kinetic effects such as, e.g., long-range order (LRO) relaxation. Most of simulation studies of structural kinetics are thus carried out by means of the MC technique (for references see numerous works of Binder, e.g., Ref. [13]). Crucial for the success of any simulation, the interatomic potential can be deduced from first-principle MD, providing an accurate description of the atomic interactions, but requiring enormous computational time and a limited number of particles. To a great extent, this limitation can be overcome by using empirical or semi-empirical potentials which have the advantage of reproducing fast and with satisfying accuracy the thermodynamic and structural properties of materials. Very

[a] e-mail: mallalen@uos.de

satisfying results have been obtained, in this way, in transition metals and alloys [14,15].

The Co-Pt system has interested many researchers from a practical viewpoint as providing catalyst materials [16], but from a basic viewpoint as a magnetic system with a coupling between chemical and magnetic ordering [17–19]. Around the 50/50 stoichiometry, CoPt orders in the $L1_0$ structure, made of alternating pure cobalt and platinum (001) planes [20]. This very anisotropic chemical order is accompanied by a strong magnetic anisotropy and a tetragonality ($c/a < 1$). The pronounced anisotropic properties of CoPt are at the core of the present renewed interest in this system [21–23]. In thin films, $L1_0$-CoPt alloys display, in addition to a high magnetic anisotropy, a magnetisation that is perpendicular to the film surface, thus making such films good candidates for magneto-optical-storage devices [24]. This system has been studied extensively to understand the origin of the asymmetry in its phase diagram. Various explanations have been proposed: for example, an effect of many-body interactions [19], an influence of magnetism, and variations of atomic interaction with composition [25,26]. Calculation of this phase diagram may appear quite simple a priori, as it is based on the fcc lattice at almost all temperatures and compositions, but it still remains a challenge today. The kinetics of atomic ordering in the ordered phases in this system has also been studied. The activation energy of changes in chemical LRO has been determined by resistivity measurements to be 3.18 eV and 2.52 eV for $CoPt_3$ [27] and CoPt [28] respectively.

It is well known, that the vacancy-driven mechanism, namely, the vacancy-atom jump between nearest-neighbours sites, is the dominant microscopic process of diffusion in dense phases [29]. During such a jump, the energy barrier formed by the nearest-neighbours that the jumping atom has to overcome for completing the jump plays an important role. In this paper, we present MD simulations based on the Tight-Binding Second Moment Approximation (TB-SMA) formalism [30], which is well adapted to transition metals and alloys [31], to calculate the saddle-point energies for the different kinds of atomic jumps. The calculated saddle-point energies will be used, in conjunction to the potentials deduced from the TB-SMA, to simulate the LRO relaxation in CoPt and deduce the migration energy using a MC technique.

2 Saddle-point energies calculation

In this section, we present the many-body potential and its parametrisation procedure. Once well defined, the potential will be used to simulate the atom-vacancy jump mechanism and deduce the energy barriers for the different kinds of atomic jumps to a nearest-neighbour vacancy in the $L1_0$-CoPt structure in the case of a rigid and a relaxed lattice.

The potential we have used is based on the approach proposed by Rosato et al. [15,32,33] where the energy E_i of an atom at site i, derived in the TB-SMA formalism [30], is written as the sum of two terms; an attractive band energy (E_i^b) and a repulsive pair interaction term (E_i^r). The band term is obtained by integrating the local density of states up to the Fermi level [34], this gives rise to the many-body character of the potential necessary to account for surface relaxations and reconstructions whereas the repulsive term is described by a sum of Born-Mayer ion-ion repulsions. When replacing the realistic density of states by a schematic rectangular one having the same second-moment [15], one obtains:

$$E_i^b = -\sqrt{\sum_{j,r_{ij}<r_c} \xi_{IJ}^2 \exp\left[-2q_{IJ}\left(\frac{r_{ij}}{r_0^{IJ}}-1\right)\right]} \quad (1)$$

and

$$E_i^r = \sum_{j,r_{ij}<r_c} A_{IJ} \exp\left[-p_{IJ}\left(\frac{r_{ij}}{r_0^{IJ}}-1\right)\right] \quad (2)$$

I and J indicate the chemical species Co or Pt. ξ_{IJ} is an effective hopping integral and q_{IJ} describes its dependence on the relative interaction distance. p_{IJ} is related to the bulk modulus of the alloy under consideration. In our case r_0^{II} is the first-neighbour distance in the metal I. r_0^{IJ} as a free parameter and it is different from the first-neighbour distance $r_0^{IJ}=(r_0^{II}+ r_0^{JJ})/2$. r_{ij} is the distance between atoms at sites i and j. E_i^b and E_i^r are cancelled beyond a cut-off radius r_c which has been chosen as the second-neighbour distance. From r_c up to the (Co-Co) third-neighbour distance, the potential is linked up to zero with a fifth-order polynomial in order to avoid discontinuities, both in the energy and in the forces. The TB-SMA potential applied to intermetallic compounds gives very reliable results with interactions up to the second nearest-neighbours as long as intermediate and low-temperature ranges are considered. Long-range interactions are required in order to reproduce high-temperature properties which are usually beyond the capability of short-range potentials. Considering the temperature range (600–980 K) and the goal of our simulations, the approximation of interactions up to the second nearest-neighbours is rather justified. Furthermore, X-ray and neutron diffuse scattering measurements have been used in conjunction with inverse cluster variation method to calculate the effective pair interactions in $L1_2$-Co_3Pt and in $L1_2$-$CoPt_3$ [25,26]. In both systems the first and second interactions are the predominant ones. The same calculations are now in progress in equiatomic CoPt [35].

The potential parameters ξ_{IJ}, A_{IJ}, p_{IJ} and q_{IJ} are a priori unknown and will be determined by fitting the potential to the universal equation of state driving the variation of the potential with distance [14]. This procedure requires usually the knowledge of the cohesive energy, lattice parameters and bulk modulus of the system. We have taken these parameters from the literature [36]. We aimed during the fit to reproduce correctly the formation energies and the lattice parameters of the ordered $L1_0$ and the disordered A_1 phases of CoPt.

The final parameters of the potential are summarised in Table 1. In Table 2, we report together the calculated

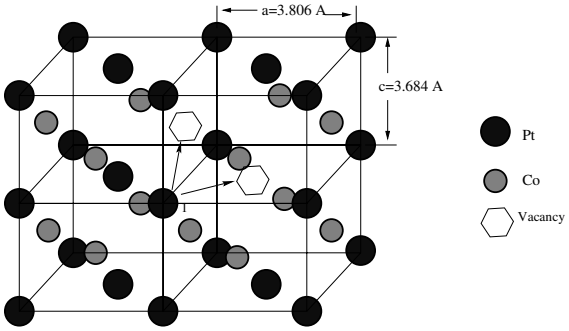

Fig. 1. The two possible atomic jumps, in-plane and out-of-plane, of the Pt atom.

Table 1. Potential parameters of inter-atomic interactions deduced from the TB-SMA. The interaction parameters between Co-Co and Pt-Pt are taken from the literature [36].

Interaction	A (eV)	ξ(eV)	p	q
Pt-Pt	0.242	2.506	11.14	3.68
Co-Co	0.189	1.907	8.8	2.96
Pt-Co	0.175	2.115	9.412	2.812

Table 2. Reduced lattice parameters, calculated (E_{cal}) and experimental (E_{exp}) formation energies of the ordered $L1_0$ and disordered A1 phases. In $L1_0$ phase, the results obtained by varying a, c, and both a and c simultaneously are shown. We have used $a_0 = 3.806$ Å, $c_0 = 3.684$ Å for the $L1_0$ phase and $a_0 = 3.751$ Å for the A1 phase.

	E_{cal} (eV)	E_{exp} (eV)	a/a_0	c/c_0
$L1_0$ (varying a)	–0.133	–0.14	0.99	
$L1_0$ (varying c)	–0.142	–0.14		0.97
$L1_0$ (varying a and c)	–0.138	–0.14	0.995	0.995
A_1 (varying a)	–0.086	–0.10	1	

lattice parameters and the formation energies and compare them to the experimental data. A good agreement is achieved for both ordered $L1_0$ and disordered A1 phases. We have attempted to parameterise the TB-SMA potential for the $L1_2$-$CoPt_3$ phase but a discrepancy of more than 40% appeared between the experimental and the calculated formation energies. For this reason, further calculations, aiming at the determination of the saddle-point energies, have been restricted to the $L1_0$ phase.

In order to calculate the saddle-point energies, we have used a simulation box containing 10^3 $L1_0$ fcc-based cells. In accord to the $L1_0$ structure, there are as many Co as Pt atoms arranged on (001) alternating crystallographic planes of pure Co and Pt using periodic boundary conditions in the three space directions. The total energy of the system, containing a single vacancy, was monitored during the four kinds of atomic jumps to a nearest-neighbour vacancy in the case of a rigid and a relaxed lattice: Co to Co-site vacancy (Co→Co(V)), Co to Pt-site vacancy (Co→Pt(V)), Pt to Pt-site vacancy (Pt→Pt(V)) and Pt to Co-site vacancy (Pt→Co(V)). In Figure 1 we represent the two possible jumps of a Pt atom toward a vacancy situated either in the same plane (Pt→Pt(V)) or in a neighbouring plane (Pt→Co(V)). In the case of a relaxed lattice, we have used a Tight Binding-Quenched Molecular Dynamics-Second Moment Approximation (TB-QMD-SMA), which allows us to determine the equilibrium structure of a system with a finite number of particles at $T = 0$ K, by integrating the equation of motion [37]. The quenching procedure, in which the velocity v_i of an atom i is cancelled when the product $F_i(t)v_i(t)$ is negative, leads to the minimisation of the potential energy at 0 K [38]. F_i being the force acting on the atom i, calculated in the extended tight-binding formalism from the total energy [34]. The positions were integrated by means of the Verlet algorithm [39]

Table 3. Calculated saddle-point energies in eV for the different kinds A→B(V) jumps of an atom A on a vacancy site B in the case of a rigid (ϵ) and a relaxed lattice (ϵ^R).

	Co→Co(V)	Co→Pt(V)	Pt→Pt(V)	Pt→Co(V)
ϵ	0.49	0.41	0.54	0.39
ϵ^R	0.39	0.34	0.42	0.31

For all atomic jumps, the total energy follows a smooth cosine curve, with a maximum close to half-way between the initial and destination lattice sites. In the case of the cross jumps, Co→Pt(V) and Pt→Co(V), a shift in the total energy, associated to the formation of an anti-site defect, was observed at the final position. The saddle-point energies have been deduced from the evolution of the total energy for the different kinds of atomic jumps. The results obtained with and without relaxation are reported in Table 3. The saddle-point energies are denoted ϵ^R and ϵ for the relaxed and the non-relaxed lattice respectively. The amplitude of the saddle-point energies may be explained by the size effect and the atoms forming the barrier of first-nearest neighbours that the jumping atom has to overcome for completing the jump. For instance, the largest value is obtained in the case of Pt→Pt(V) jump, when the bigger Pt atom is involved in the jump. In the case of the cross jumps, Co→Pt(V) and Pt→Co(V), the atomic structure of the barrier to overcome being the same for the two jumps, the corresponding saddle-point energies are very close. Furthermore, the lattice being softer when relaxed, the saddle-point energies, are as expected, smaller when the relaxation is taken into account.

3 Monte Carlo simulations

3.1 Simulation method

MC simulations have been established as a useful tool for studying order-order and order-disorder relaxation kinetics in intermetallics [40–42]. In contrast to earlier studies, based on effective pair interaction energies expressed within a simple Ising-Hamiltonian, we go in the present work beyond the pair approximation by implementing the many-body potential deduced from the TB-SMA and taking into account the saddle-point energies calculated in the

previous section to simulate the disordering process of a perfectly ordered $L1_0$-CoPt structure. The purpose of the simulation is to prove whether the interaction model is appropriate and to get an estimation of the vacancy migration energy which is an important energetic parameter that drives diffusion and ordering process in intermetallics.

In view of recent neutron diffuse scattering measurement in equiatomic CoPt [35] which show a symmetric distribution of the diffuse intensity around the 100 and equivalent points in the reciprocal lattice, signature of a highly stable $L1_0$ phase with very small static displacements, we have chosen to carry on the MC simulations using a rigid lattice. We have used a model based on the vacancy-atom jump mechanism between nearest-neighbour sites, which is the realistic microscopic process in dense phases [29]. The simulation box contains 32^3 $L1_0$ fcc-based cells with linear periodic boundary conditions. The simulation starts with a perfect $L1_0$ ordered crystal in which one of the two sublattices (sublattice α) is occupied by Co atoms and the other (sublattice β) by Pt atoms. To not affect the static properties and avoid interaction effects, a single vacancy is introduced at random in the crystal. The elementary MC step is the following: one of the vacancy neighbours (Co or Pt atom) is randomly chosen, the energy balance ΔE of the atom-vacancy exchange before and after the jump is evaluated. The jump is performed if the Glauber probability $P(\Delta E) = P^G(\Delta E)\exp(-\epsilon/k_BT)$ is larger than a random number between 0 and 1. $P^G(\Delta E) = [1+\exp(\Delta E/k_BT)]^{-1}$ is the Glauber probability [43] and ϵ is the saddle-point energy for the corresponding jump. This corresponds to averaging the result over a large number of reversal jump attempts, the sum of the probabilities of the jump and its reversal being equal to 1.

The configuration of the system was analysed, at regular time intervals, by calculating the LRO parameter $\eta = 2(2N^{\alpha}_{\mathrm{Co}} - N_{\mathrm{Co}})/(N_{\mathrm{sites}} - 1)$, where N^{α}_{Co} is the number of Co atoms on the α sublattice and N_{Co} the total number of Co atoms. The time scale being the number of jump attempts. For each temperature, the evolution of η is followed until the system reaches equilibrium. We have chosen to stop when the simulation time was at least longer than 5 times the relaxation time of the system.

3.2 Results and discussion

Isothermal relaxations of η have been recorded in the temperature range from 600 to 980 K. An example of kinetics relaxation is shown in Figure 2. According to the path probability method [44], corroborated by many experimental results [45–49], the isothermal relaxation of the LRO parameter in intermetallics is well fitted with two exponentials, yielding a long and a short relaxation times, corresponding to the slow and the fast processes, respectively. This result is well established in $L1_2$ phase for which a detailed study has shown that the fast process is related to the formation of the nearest-neighbour antisite pairs, whereas the slow one is related to the uncoupling of these antisite pairs [40]. Due to the difference in structure, the process must be different in the $L1_0$ phase and

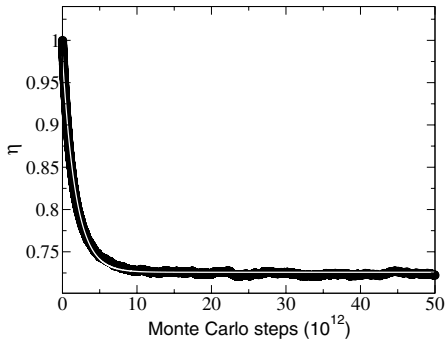

Fig. 2. Isothermal relaxation of η obtained for $T = 880$ K (black circles) and its simulation using a single exponential (white line).

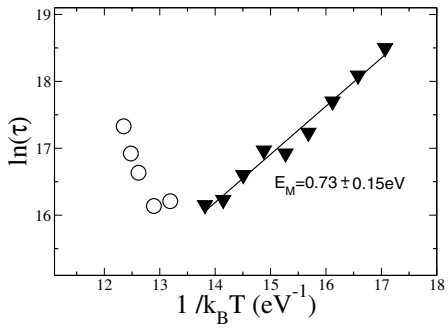

Fig. 3. Arrhenius plot of the relaxation times. The linear regression gives the migration energy $E_M = 0.73 \pm 0.15$ eV. The open circles show the data points which have been excluded from the linear regression.

the interpretation is still under investigation. However, recent MC simulations of the LRO relaxation in $L1_0$-FePd showed that the fast process is highly predominant (up to 90%) below the order-disorder transition [50]. In view of these results and considering the temperature range of our simulations, we have chosen to fit the kinetics using a single exponential yielding a single relaxation time τ which fulfils an Arrhenius law with a positive migration energy $E_M = 0.73 \pm 0.15$ eV (Fig. 3). The relaxation times are typically in the order of 10^{12} MC steps, significantly higher than the relaxation times obtained without saddle-point energies. The data points on the left side of Figure 3, plotted in open circles, show a clear departure from the straight line, they are synonym of a critical slowing down close to the order-disorder transition and have been excluded from the linear regression.

The vacancy formation energy E_F has been measured in pure Co and pure Pt, it has been found equal to 1.38 eV and 1.2 eV for Co and Pt respectively [51]. Assuming that the activation energy E_A is the sum of E_M and E_F, the calculated value of E_A obtained considering the simulated value of E_M and an average value of E_F compares well to the activation energy of 2.52 eV, measured in equiatomic CoPt by means of resistivity measurements [28]. Normal modes of vibration in equiatomic CoPt have been recently measured by inelastic neutron scattering [52]. The phonon

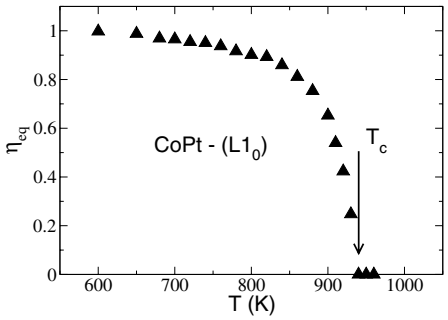

Fig. 4. Temperature variation of the equilibrium LRO parameter η_{eq}.

density of states has been used to calculate the migration energy using Schober's model. A value of 0.85 eV was found in the fcc-disordered state at 1120 K. Despite of the difference in the state of order between the simulated CoPt system and the measured one, the qualitative agreement is quite satisfactory. In our knowledge no further measurement of the migration energy in equiatomic CoPt are available. Nevertheless, qualitative comparison to $CoPt_3$, in which the migration energy was calculated using both Schober's and Flynn's models, can be made.

Schober's model initially developed for bcc and fcc pure metals [10] has been extended to the A_3B compounds with $L1_2$ structure [11] and applied to $CoPt_3$ [53]. Averaging the values of the migration energy over the different kinds of atomic jumps, we get a migration energy of 1.3 eV at 300 K. Flynn's model [9] was applied to $CoPt_3$ using the elastic constants deduced from the slope of the phonon dispersion curves at the center of the Brillouin zone [53]. A migration energy of 0.95 eV was found in the fcc-disordered state at 1060 K. The difference in the amplitude between the calculated value of the migration energy in CoPt and the values deduced from Schober's and Flynn's models in $CoPt_3$ might be explained by the atomic mass and size effects. As expected, an increase in the migration energy with the atomic density is observed between the $L1_0$ and $L1_2$ phases of Co–Pt system. The atomic density is nearly 25% lower in CoPt than in $CoPt_3$.

The variation of the equilibrium LRO parameter η_{eq} as a function of temperature is shown in Figure 4. The order-disorder transition takes place between 930 and 935 K. The transition region has been crossed with 5 K temperature steps. It should be noted that the value of this temperature is close to the value obtained in the $L1_0$ compounds using phenomenological pair interaction energies [54] but it is 15% lower than the experimental value of the order-disorder transition temperature T_c in equiatomic CoPt (1110 K) [55]. Nevetheless, the general agreement between the simulated and the experimental T_c is quite satisfactory. In fact, the MC model, which assumes temperature independent potentials and does not take into account anti-phase domains, only gives an estimate of T_c. Indeed, recent X-ray diffraction and transmission electron microscopy measurements in CoPt showed that the ordering transformation involves formation of antiphase boundaries and twin bands [17].

4 Conclusion

An approach for determining the parameters of a many-body potential in equiatomic CoPt using the TB-SMA has been presented. The potential was used to determine the saddle-point energies for the different kinds of nearest-neighbour atom-vacancy jumps in the case of a rigid and a relaxed lattice. The calculated energy barriers have been used together with the many-body potential to simulate the LRO relaxation in $L1_0$-CoPt structure using a MC technique. A vacancy migration energy of 0.73 ± 0.15 eV has been deduced from the Arrhenius plot of the relaxation times. A lack in experimental data of the migration energy in the ordered state of the equiatomic CoPt made possible only qualitative comparisons to either the disordered state of CoPt data, when available, or to $CoPt_3$ data. Finally, the order-disorder transition temperature has been determined from the isothermal relaxation of the LRO parameter. The simulated value is in a satisfactory agreement with experiment.

This work was supported partly by the Algerian Project ANDRU/PNR3 and by the collaborative program 99 MDU 449 between the University Mouloud Mammeri of Tizi-Ouzou, Algeria and the University Louis Pasteur of Strasbourg, France. The authors would like to thank Pr. Treglia, Dr. Goyhenex and Dr. Pierron-Bohnes who provided us with the initial MD code.

References

1. G.R. Harp, D. Weller, T.A. Rabedeau, R.F.C. Farrow, M.F. Toney, Phys. Rev. Lett. **71**, 2493 (1993)
2. A. Cebollada, D. Weller, J. Sticht, G.R. Harp, R.F.C. Farrow, R.F. Marks, R. Savoy, J.C. Scott, Phys. Rev. B **50**, 3419 (1994)
3. O. Ersen, V. Parasote, V. Pierron-Bohnes, M.C. Cadeville, C. Ulhaq-Bouillet, J. Appl. Phys. **93**, 2987 (2003)
4. V. Gehanno, A. Marty, B. Gilles, Y. Samson, Phys. Rev. B **55**, 12552 (1997)
5. P. Kamp, A. Marty, B. Gilles, R. Hoffmann, S. Marchesini, M. Belakhovsky, C. Boeglin, H.A. Dürr, S.S. Dhesi, G. van der Laan, A. Rogalev, Phys. Rev. B **59**, 1105 (1999)
6. H. Schultz, in *Atomic Defects in Metals*, Landolt-Börnstein, New Series, Group III, Vol. 25, edited by H. Ullmaier (Springer, Berlin, 1991)
7. E. Balanzat, J. Hillairet, J. Phys. F: Met. Phys. **11**, 1977 (1981)
8. A. Schulze, K. Lücke, Acta Metall. **20**, 529 (1972)
9. C.P. Flynn, Phys. Rev. **171**, 682 (1968)
10. H.R. Schober, W. Petry, J. Trampenau, J. Phys.: Condens. Matter **4**, 9321 (1992)
11. E. Kentzinger, H.R. Schober, J. Phys.: Condens. Matter **12**, 8145 (2000)
12. F. Willaime, C. Massobrio, in *Defects in Materials*, edited by P.D. Bristome et al., MRS Symposia Proceedings No. 209 (Materials Research Society, Pittsburgh, 1991), p. 293

13. K. Binder, *Monte Carlo Methods in Statistical Physics*, edited by K. Binder (Springer Berlin, 1979)
14. F. Cleri, V. Rosato, Phys. Rev. B **48**, 22 (1993)
15. V. Rosato, B. Guillope, B. Legrand, Philos. Mag. A **59**, 321 (1989)
16. S. Zyade, F. Garin, G. Maire, New J. Chem. **11**, 429 (1987)
17. Q.F. Xiao, Z.D. Zhang, F.R. de Boer, K.H.J. Buschow, J. All. Comp. **364**, 64 (2004)
18. M.C. Cadeville, J.L. Moran-Lopez, Phys. Rep. **153**, 331 (1987)
19. J.M. Sanchez, J.L. Moran-Lopez, C. Leroux, M.C. Cadeville, J. Phys. C **21**, L1091 (1988); J.M. Sanchez, J.L. Moran-Lopez, C. Leroux, M.C. Cadeville, J. Phys.: Condens. Matter **1**, 491 (1988)
20. T. Massalski, *Binary Alloy Phase Diagrams* (American Society for Metals, Metals Park, OA, 1990), Vol. 2
21. L. Uba, S. Uba, V.N. Antonov, A.N. Yaresko, R. Gontarz, Phys. Rev. B. **64**, 125105 (2001)
22. M. Maret, M.C. Cadeville, W. Staiger, E. Beaurepaire, R. Poinsot, A. Herr, Thin Solid Films **275**, 224 (1996)
23. K. Wantanabe, H. Masumoto, Trans. Jpn. Inst. Met. **24**, 627 (1983)
24. S. Shiomi, T. Nakakita, T. Kobayashi, M. Masuda, Jpn. J. Appl. Phys. Part 2 **32**. L1058 (1993)
25. M.J. Capitan, S. Lefebvre, Y. Calvayrac, M. Bessière, P. Cénédèse, J. Appl. Crystallogr. **32**, 1039 (1999)
26. E. Kentzinger, V. Parasote, V. Pierron-Bohnes, J.F. Lami, M.C. Cadeville, J.M. Sanchez, R. Caudron, B. Beuneu, Phys. Rev. B **61**, 14975 (2000)
27. C.E. Dahmani, M.C. Cadeville, V. Pierron-Bohnes, Acta Metall. **3**, 369 (1985)
28. J. Orehotsky, J.L. Orehotsky, J. Appl. Phys. **61**, 1210 (1987)
29. W. Petry, A. Heiming, C. Herzig, J. Trampenau, Defect. Diffus. Forum **75**, 211 (1991)
30. D. Tomanek, S. Mukherjee, K.H. Bennemann, Phys. Rev. B **28**, 665 (1983)
31. F. Ducastelle, J. Phys. France **31**, 1055 (1970)
32. M. Guillopé, B. Legrand, Surf. Sci. **215**, 577 (1989)
33. G. Tréglia, B. Legrand, F. Ducastelle, Europhys. Lett. **7**, 575 (1988)
34. J. Friedel, *The Physics of Metals*, edited by J.M. Ziman (Cambrige University Press, Cambridge, 1969)
35. M. Hamidi, Ph.D. thesis, in progress, Mouloud Mammeri University, Algeria
36. C. Goyhenex, H. Bulou, J.P. Deville, G. Tréglia, Phys. Rev. B **60**, 2781 (1999)
37. C.H. Bennett, in *The Physics of Metals*, edited by J.M. Ziman (Cambridge University Press, Cambridge, 1969), p. 340
38. C.H. Bennett, in *Diffusion in Solids, Recent Developments*, edited by A.S. Nowick, J.J Burton (Academic New York, 1975), p. 73
39. L. Verlet, Phys. Rev. **159**, 98 (1967)
40. P. Oramus, R. Kozubski, V. Pierron-Bohnes, M.C. Cadeville, W. Pfeiler, Phys. Rev. B **63**, 174109 (2001)
41. R. Kozubski, P. Oramus, W. Pfeiler, M.C. Cadeville, V. Pierron-Bohnes, C. Massobrio, Arch. Metall. **46**, 145 (2001)
42. A. Kerrache, H. Bouzar, M. Zemirli, V. Pierron-Bohnes, M.C. Cadeville, M.A. Khan, Comp. Mater. Sci. **17**, 324 (2000); A. Kerrache, H. Bouzar, M. Zemirli, V. Pierron-Bohnes, M.C. Cadeville, M.A. Khan, in *Proceedings of DIMAT 2000*, edited by Y. Limoge, J.L. Bocquet (Scitec, Uetikon-Zürich, 2001), pp. 403–409
43. R.J. Glauber, J. Math. Phys. **4** (1963)
44. H. Sato, K. Gschwend, R. Kikuchi, J. Phys. C **7**, 357 (1991)
45. C. Dimitrov, T. Tarfa, O. Dimitrov, in *Ordering and Disordering in Alloys*, edited by A.R. Yavari, (Elsevier Barking, 1992), p. 130
46. R. Kozubski, W. Pfeiler, Acta. Mater. **44**, 1573 (1996)
47. H. Lang, H. Uzawa, T. Mohri, W. Pfeiler, Intermetallics **9**, 9 (2001)
48. G. Sattonay, O. Dimitrov, Acta. Mater. **47**, 2077 (1999)
49. A. Kulovits, W.A. Soffa, W. Püschl, W. Pfeiler Mater. Res. Soc. Symp. Proc. B **5**, 753 (2003)
50. T. Mehaddene, O. Adjaoud, R. Kozubski, K. Tanaka, H. Numakura, J.M. Sanchez, Ch. Issro, W. Pfeiler, V. Pierron-Bohnes, Scripta Mater. **53**, 435 (2005)
51. H.J. Wollenberger, in *Physical Metallurgy*, 3rd edn., edited by R.W. Cahn, P. Haasen (Elsevier, Amesterdam, 1983)
52. L. Messad, B. Hennion, T. Mehaddene, V. Pierron-Bohnes, private communication
53. T. Mehaddene, E. Kentzinger, B. Hennion, K. Tanaka, H. Numakura, A. Marty, V. Parasote, M.C. Cadeville, M. Zemirli, V. Pierron-Bohnes, Phys. Rev. B **69**, 024304 (2004)
54. A. Kerrache, Magister thesis, Mouloud Mammeri University, Algeria (2000)
55. C.E. Dahmani, M.C. Cadeville, V. Pierron-Bohnes, Acta Metall. Mater. **33**, 369 (1985)